Developing tamoxifen-based chemical probes for use with a dual-modality fluorescence and optical coherence tomography imaging needle

Louisa A. Ho,[a] Loretta Scolaro,[b,c,d] Elizabeth Thomas,[e] Bryden C. Quirk,[b,c,d] Rodney W. Kirk,[b,c,d] Robert A. McLaughlin,[b,c,d] and Rebecca O. Fuller[a,f,g] *

[a] School of Molecular Sciences M310, The University of Western Australia, 35 Stirling Hwy, Crawley WA 6009, Australia.

[b] Australian Research Council Centre of Excellence for Nanoscale Biophotonics, Adelaide Medical School, The University of Adelaide, North Terrace, Adelaide SA 5005, Australia.

[c] Institute for Photonics and Advanced Sensing, The University of Adelaide, North Terrace, Adelaide SA 5005, Australia.

[d] School of Electrical, Electronic and Computer Engineering, The University of Western Australia, 35 Stirling Hwy, Crawley WA 6009, Australia.

[e] School of Surgery M507, The University of Western Australia, QEII Medical Center, Monash Ave, Nedlands, WA 6009, Australia.

[f] School of Molecular and Life Sciences, Curtin University, Bentley WA 6102, Australia.

[g] Current address, School of Natural Sciences-Chemistry, University of Tasmania, Hobart, Tasmania 7001, Australia

*Corresponding author email address: rebecca.fuller@utas.edu.au

Abstract

Fluorescent small molecules based on the chemotherapeutic tamoxifen have been synthesised for use with an imaging needle capable of acquiring simultaneous fluorescence and optical coherence tomography (OCT) images. The chemical probes are based on the active metabolite of the drug, 4-hydroxytamoxifen that is coupled with a diamine linker to commercially available Alexa Fluor™ or BODIPY dyes. The tamoxifen derivatives were then added to cultures of live estrogen receptor positive MCF-7 human breast cancer cells and imaged using the miniaturised fibre-optic device enclosed within a 23-gauge needle (outer diameter 640μm). The OCT images showed the micro-architecture of the cell culture, while the fluorescence identified estrogen receptor positive cell. Both dyes were found to have suitable excitation and emission properties and are good candidates to further develop as probes for fluorescence-guided surgery.

Introduction

The development of small molecule fluorescent probes is a significant area of current interest.[1-3] Molecules that have the ability to bind to specific target receptors in cells provide the promise of imaging at a molecular level. Research is often focused on the development of new probes that are selective to specific cellular processes and properties, providing a means for scientists to understand the mechanisms behind key biological processes through the visualisation and quantification of cellular features such as nucleic acids, proteins and ions.[1] Some of the most highly anticipated fluorescent probes are for the detection of cancer and its associated processes.

Tamoxifen is a small molecule (Figure 1) that has become an essential component in the prevention and treatment of breast cancer. The drug was the first therapeutic that targeted estrogen receptor (ER) positive tumors.[4] Being a selective drug, it only modulates the estrogen receptors.[5] It is one of the success stories in medical oncology, finding widespread use in a variety of treatment and preventative measures.[6] This molecule is an ideal candidate for further development, both in terms of improving the therapeutic potential as well as for use as a chemical probe. Indeed, many new examples are being developed for a variety of uses.[7-8] Despite this potential, there are very few examples of fluorescent analogues that are reported in the literature.[9-11]

The development of small molecule fluorescent probes for cancer detection is not a new idea. A large body of research into the synthesis of these materials already exists.[12-13] Probes are developed for use both in laboratories as well as in clinical applications.[3, 14] One underrepresented area of this research is the use of molecular probes in fluorescence-guided surgery.[15] We aim to build on this through use of a fluorescent probe paired with an intraoperative imaging device to improve the accuracy of breast cancer surgery.

In particular, our goal is to produce a conjugate of tamoxifen that targets the estrogen receptors, and demonstrate that it may be imaged with a dual-modality fluorescence + optical coherence tomography (OCT) device. OCT is an imaging modality commonly used in ophthalmology[16] and cardiology.[17-18] It provides label-free images of tissue micro-architecture, typically at a spatial resolution of 5 to 20μm. OCT is based on detection of back-scattered near-infrared light using low-coherence interferometry.[19] While its use has been explored in breast cancer,[20] it suffers poor tissue differentiation because several tissues present in breast cancer have similar optical scattering and

absorption properties. The simultaneous detection of a cancer-specific fluorescent probe would significantly improve tissue differentiation, whilst complementing the ability of OCT to image the structural organisation of the tissues.

Utilising optical imaging in a solid tissue cancer such as breast cancer is limited by the poor image penetration of optical techniques in turbid tissue. Techniques such as fluorescence and OCT are typically limited to a few hundred microns up to 1.5mm.[21-22] To address this, we will make use of an *imaging needle* (Figure 2).[23-24] The device consists of an optical fibre with a miniaturised lens fabricated at the distal end.[25] The optical fibre transmits and detects the imaging light (both OCT and fluorescence). This is enclosed within a 23-gauge needle (outer diameter 640µm). By incorporating the imaging device into a small, rigid needle, we are able to insert it deep within tissue, well beyond the image penetration depth that typically limits optical imaging techniques. This provides a technical pathway to utilise such imaging techniques intra-operatively for the detection of residual malignant tissue following surgical excision of the tumour.[26] One application of such a tool is to reduce the incidence of involved margins in breast cancer surgery, and thus reduce the proportion of patients who are required to undergo additional surgery.

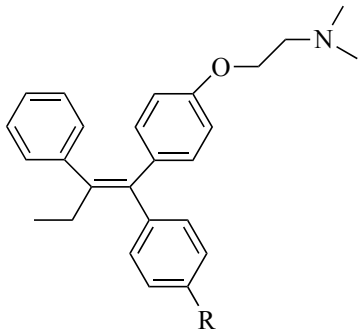

Figure 1: The chemical structure of the drug tamoxifen (R=H) and the active metabolite 4-hydroxytamoxifen (R=OH).

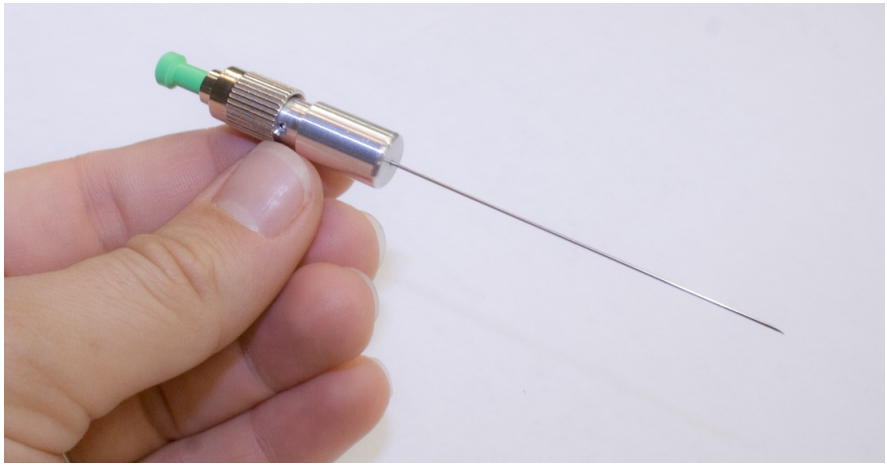

Figure 2:Imaging needle (diameter 640 µm).

This proof of concept study involves using the imaging needle to detect small molecule fluorescent probes in cell lines. The chemical probe is based on the active metabolite of the drug tamoxifen, 4-hydroxytamoxifen (Figure 1) that is known to work by inhibiting the growth of ER cells that account for 75% of breast cancer cases.

To date, a number of tamoxifen analogues that have the ability to conjugate to fluorophores have been developed by the wider scientific community to be used to study estrogen receptor mediated processes both inside and outside of the cells using confocal microscopy.[9-11] We have aimed to develop a new analogue to test the suitability of this small molecule as a contrast agent for use with the dual-modality imaging needle. In particular, we have conjugated 4-hydroxytamoxifen to one of the brightest and most stable fluorophores (FL) that minimises self-quenching, an Alexa Fluor™ 488 dye (AF488). This dye was chosen to maximise our likelihood of observing the cells during imaging with the imaging needle. We have also prepared a previously reported[9] analogue using the more economic and widely used BODIPY FL. While both dyes have similar excitation and emission profiles, they differ in cell permeability. The Alexa Fluor™ dyes are cell impermeable, and unlike the BODIPY FL may lack the ability to enter the cell and interact with the ER. The two analogues provide scope to determine which FL is more suitable for use with an imaging needle.

Results and discussion

Synthesis of the new compound, **4** is based on two previously reported methods (Scheme 1).[9, 27] Briefly the estrogen modulator, 4-hydroxytamoxifen was made through a McMurry coupling reaction. The amine containing basic side chain is known to extend out of the binding pocket of the estrogen receptor alpha, hence a useful group to modify for conjugation.[28] In this case, the triphenylethylethylene **(1)** is monoalklylated with dibromoethane **(2)**. A mixture of the E and Z isomers is produced from the reaction. Although it is the Z isomer which predominantly is found to bind to the receptor both *in vivo* and *in vitro*.[29] It has been shown in pure (99 %) hydroxytamoxifen isomers that they undergo facile isomerisation in tissue culture medium at 37 ^{o}C.[29] Despite the mixture of isomers produced in this work, there should be sufficient quantities of the active trans form of the metabolite for binding. Nucleophilic substitution of the haloalkane with diaminohexane is then used to provide a spacer group **(3)** for conjugation of the fluorophore AF488 to the small molecule **(4)**. A second analogue was also prepared **(5)**, only differing from complex **4** in the final conjugation step, which involved an alternative dye BODIPY FL. Cell lines were incubated with **4** and **5** using conditions developed previously.[11]

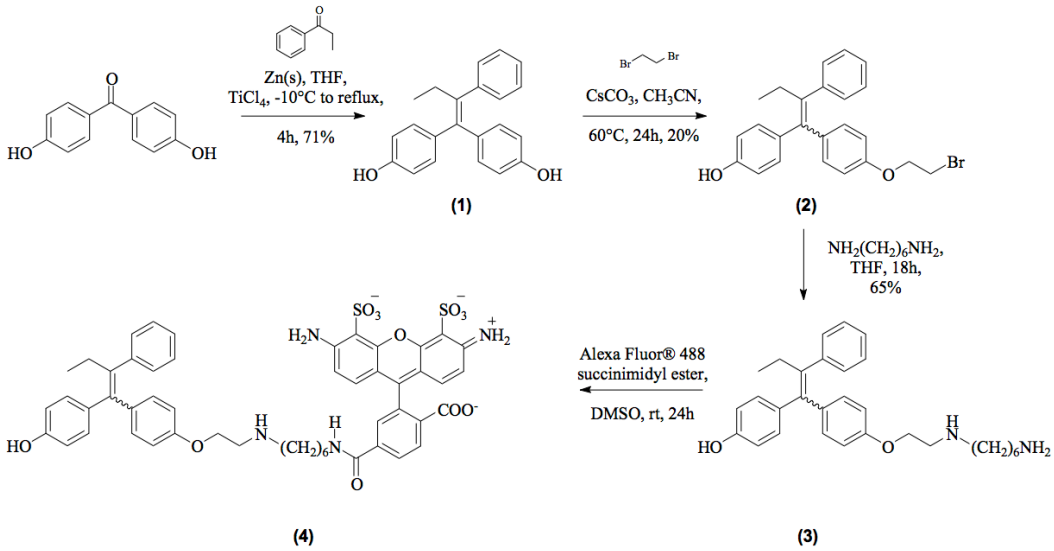

*Scheme 1: Synthesis of the AF488 conjugate of 4-hydroxytamoxifen **(4)**.*

The cellular localisation of **4** with ER-positive MCF7 breast cell lines was initially visualised by fluorescent confocal microscopy (Figure 3). A bright field confocal image for the control MCF7 cell lines has been included in the supplementary information (Fig S1). Following incubation of the cells with the conjugate, uptake studies found the molecule was associated with the cells. **4** uses a cell-impermeable fluorescent dye, AF488, meaning it is unlikely to be internalised. Indeed, localisation appears to be consistent with a similar literature example involving the Alexa Fluor™ 546 dye.[9] Cellular uptake of conjugate **5** was consistent with previous literature reports,[9] it maintains the ability to bind to ER alphas cells with similar localisation to **4**. Experiments were also conducted with ER-negative (MDA231) cell lines (Fig. S2 and S3). Others have seen that there is no specificity for compound **5** nor an alternative Alexa Fluor™ analogue.[9] We also find there is no selectivity using either compound **4** or **5**. This is likely the result of the hydrophobic linker used to conjugate the fluorophore to the tamoxifen and in the case of **4**, the impermeable nature of AF488. Nonetheless, both compounds still demonstrate that fluorescent analogues of tamoxifen maybe visualised with the highly miniaturised optics present in an imaging needle.

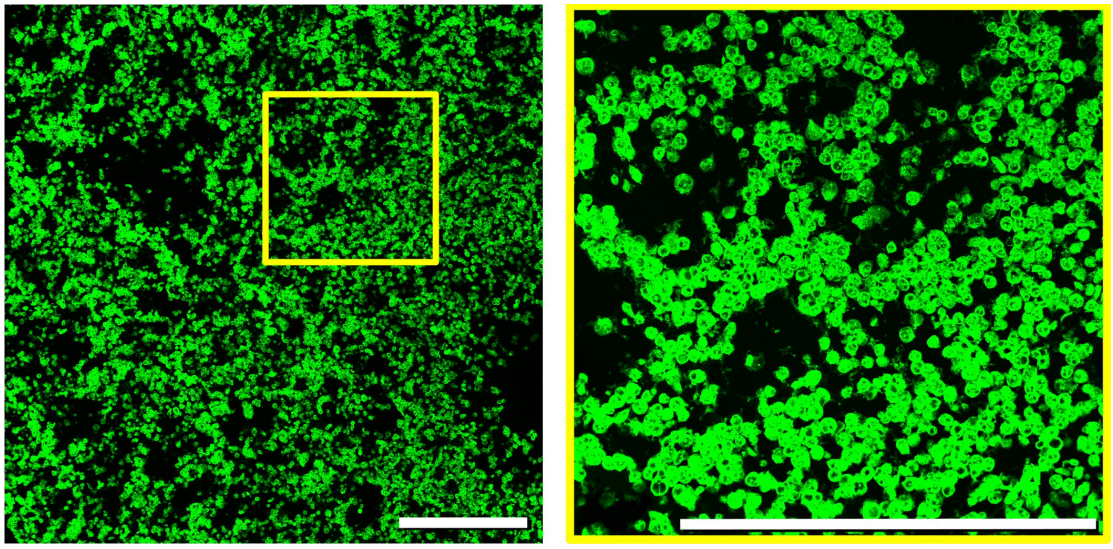

*Figure 3: Wide field fluorescence images of ER-positive MCF7 cell lines following incubation with conjugate for 1 hour of dosing with 10 μM of **4**; Scale bar 0.5 mm.*

Figure 4 shows images acquired by positioning and translating the imaging needle a few hundred microns above cell plates containing ER-positive MCF7 cell lines which were either unlabelled (control, top row of Figure 4) or had been incubated with **4** (bottom row of Figure 4). Both OCT and fluorescence images were acquired simultaneously through the same focusing optics and so are intrinsically co-registered. In the OCT image, cells appear as localised areas of high optical backscatter (light grey) and show the structure of the cell culture. Individual cells can be seen in areas of low concentration (bottom left corner of each image). The OCT shows that both control and labelled cells were successfully cultured. In the unlabelled experiment, fluorescence is not observed, consistent with the nature of the sample. For the cell lines that have been incubated in **4** the areas of fluorescence are consistent with the OCT image. The gradual variation in the level of fluorescence is due to a slight experimental misalignment of the imaging needle with the cell plate, such that some areas were located further from the imaging needle.

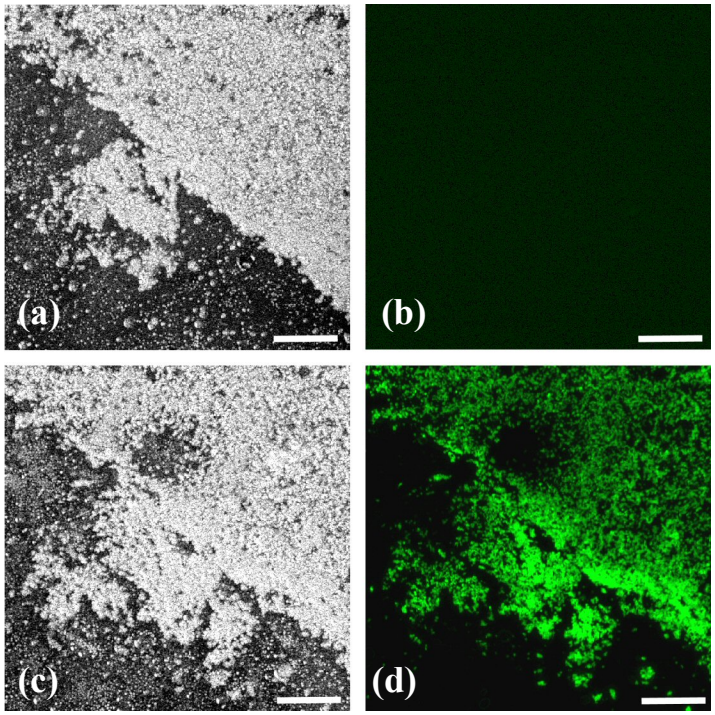

*Figure 4: (Colour online) (a, c) Structural OCT images and (b, d) corresponding fluorescence signal in the same sample. (top row) Control ER-positive MCF7 cell lines. (bottom row) ER-positive MCF7 cell lines that have been incubated with **4**. Scale bar is 0.5 mm.*

Further experiments were conducted using the imaging needle to image ER-positive MCF7 cell lines incubated with the BODIPY based conjugate, **5**. Figure 5 shows unlabelled, control samples (top row) and cells that have been incubated with **5**. Similar results to those from the AF488 conjugate **4** are shown, with no fluorescence detected in the control samples, and a clear correspondence in the labelled sample between the location of cells in the OCT and the fluorescence signal. We find that the conjugated BODIPY FL is sufficiently emissive enough to be detected with the imaging needle.

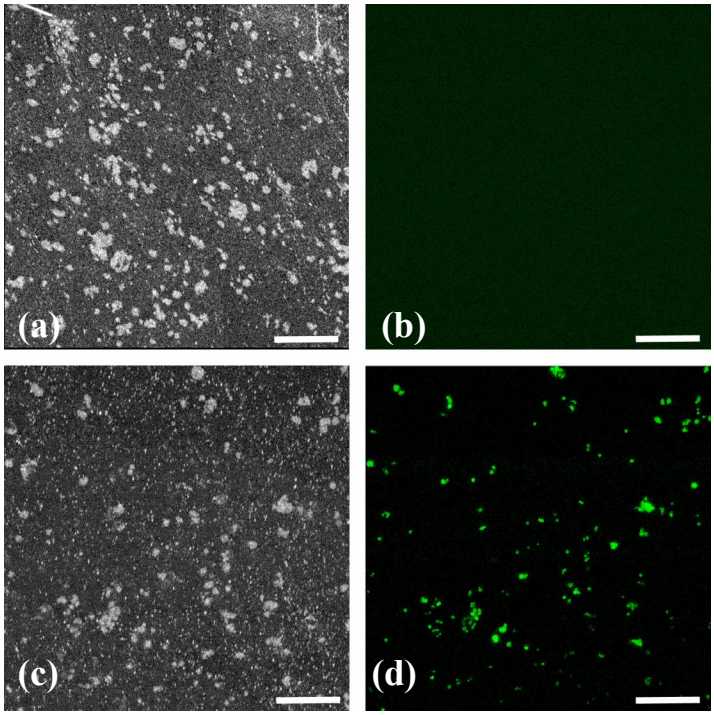

*Figure 5: (Colour online) (a, c) Structural OCT images and (b, d) corresponding projected fluorescence signal in the same sample. (top row) Control ER-positive MCF7 cell lines. (bottom row) ER-positive MCF7 cell lines that have been incubated with **5**. Scale bar is 0.5 mm.*

A co-registered multi-modal image, showing an overlay of the structural OCT and fluorescence images is shown in Figure 6. This image was obtained from ER positive cell lines incubated with **5** and shows the powerful nature of multi-modal imaging technique. These experiments provide some of the first steps to developing a contrast medium that could be used in conjunction with imaging needle for the detection of trace amounts of breast cancer following surgical excision of a tumour.

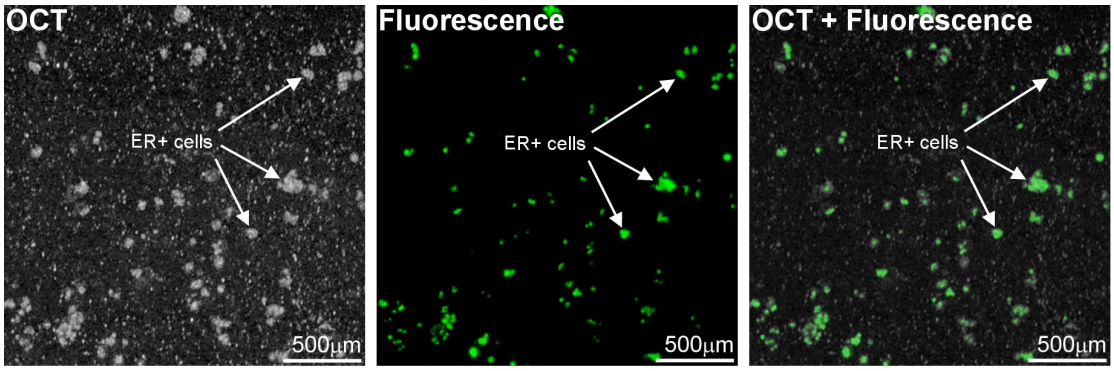

*Figure 6: ER-positive MCF7 cell lines that have been incubated with **5**. The OCT, fluorescence and combined images are shown. Labelled cells provide a point of reference for the images. Note that the other areas of fluorescence also indicate the presence of MCF7 cells.*

Previous work with dual-modality imaging needles involved detecting fluorescently labelled antibodies in human and mouse liver samples.[24] However, there has been no demonstration of the effectiveness of imaging needles to detect small molecules targeting specific receptors, as is commonly used in cancer diagnostics and therapeutics. Uncertainty in the detectability of cells incubated with a fluorescent small molecule probe warranted the synthesis of a molecular system conjugated to the most emissive dye (AF488) suitable with the needle probe. From the results presented in Figures 4 and 5, we can conclude that the use of the more cost effective and cell permeable BODIPY FL will be suitable for future work. Future work will involve experiments with an imaging needle using a selective small molecule in a wider range of cells.

Conclusion

Small molecule fluorescent probes have significant potential for intraoperative identification of tumor margins during surgery. In this work we have taken the first steps towards the goal of developing a fluorescent probe for use with an imaging needle with the potential to visualize the borders of tumors and normal tissue. We have synthesised two fluorescent tamoxifen analogues based on the conjugation of 4-hydroxytamoxifen with either the AF488 or BODIPY FL dye. These molecular probes where used to label MCF-7 human breast cells and were then imaged with a dual-modality fluorescence + OCT imaging needle. Our results showed that the miniaturised optics in the imaging needle were able to successfully detect both fluorophores and the florescence signal corresponded closely to the structural OCT images of the cell cultures.

Experimental

General experimental

All reactions were carried out under an argon gas atmosphere in flame-dried glassware with magnetic stirring, unless otherwise stated. All reaction temperatures refer to bath temperatures. All reactions involving heating were placed into a preheated oil bath at the specified temperature, unless otherwise stated. Solvents were used dry, unless otherwise stated. Solvents were dried and purified according to the methods described by Armarego W. L. K. and Chai C. In Purification of Laboratory Chemicals 5th ed.; Butterworth-Heinemann: Cornwall, 2003. All reagents were purchased from Sigma-Aldrich, Fluka, Merck, or Boron Molecular and used without further purification, unless otherwise stated. Thin layer chromatography (TLC) was performed on Merck silica gel 60 F_{254} pre-coated aluminium sheets. Visualisation of developed plates was achieved through the use of a 254 nm or 365 nm UV lamp or staining with phosphomolybdic acid stain solution. Column chromatography was performed using silica gel 60 (0.063-0.200 nm) as supplied by Merck, unless otherwise stated. HPLC was conducted using an Agilent 1200 with a photodiode array detector (PDA). Separation was achieved using a 250 × 10 mm i.d., 5 μm, Apollo C_{18} reversed phase column (Grace-Division) with a 33 mm × 7 mm guard column of the same material. The detection wavelength was set at 260 and 485 nm. ^{1}H and ^{13}C NMR spectra were acquired in the specified deuterated solvent using either a Bruker AV600 (600.13 MHz for ^{1}H and 150.9 MHz for ^{13}C), a Bruker AV500 (500.13 MHz for ^{1}H and 125.8 MHz for ^{13}C), or a Varian Gemini-400 (399.85 MHz for ^{1}H and

100.5 MHz for ^{13}C) spectrometer at 25°C. Chemical shifts are reported in parts per million downfield from tetramethylsilane using the solvent resonance as internal standard.[30] Data are reported as follows: chemical shift, multiplicity (app = apparent, s = singlet, d = doublet, t = triplet, q = quartet, m = multiplet, br = broad, sept = septet), coupling constant, integration, and assignment. Mass spectra were acquired on a Waters liquid chromatograph premier (LCT) mass spectrometer through atmospheric pressure chemical ionisation (APCI) or electrospray ionisation (ES).

1,1-Bis(4,hydroxyphenyl)-2-phenylbut-1-ene (1): Zinc powder (6.12 g, 0.094 mol) and dry THF (60 mL) were transferred to a flame-dried flask fitted with a magnetic stirrer bar, reflux condenser and dropping funnel, under argon gas. The reaction mixture was then cooled to -10°C in a carefully maintained dry ice/acetone bath. To the cooled mixture was added $TiCl_4$ (5.0 mL, 8.65 g, 0.046 mol), drop-wise. After the addition was complete, the reaction mixture was heated at reflux for 2 hours. After this time, the reaction mixture was cooled in an ice bath, and a solution of ice bath cooled 4,4'-hydroxybenzophenone (1.5 g, 0.007 mol), propiophenone (3.0 mL, 3.0 g, 0.022 mol) and dry THF (120 mL) was added *via* cannula. The resulting mixture was then refluxed for a further 2 hours in the dark. After being cooled to room temperature the reaction mixture was quenched with 10% aqueous potassium carbonate (90 mL) and then extracted with ethyl acetate (2 × 90 mL). The combined organic layers were washed with brine (90 mL), dried over $MgSO_4$, and concentrated under reduced pressure. The crude reaction mixture was then subjected to flash column chromatography (5:95 → 20:80 ethyl acetate/hexanes) to give **(1)** as a white solid (1.50 g, 71%). The spectroscopic data for compound **(1)** matched that reported previously in the literature.[27]

***E* and *Z* 4-{1-[4-(2-Bromo-ethoxy)-phenyl]-2-phenyl-but-1-enyl}-phenol (2):** A solution of **(1)** (1.5 g, 0.005 mol), cesium carbonate (9.48 g, 0.029 mol) and A.R. acetonitrile (60 mL) was heated at 60°C for 15 minutes, under an atmosphere of argon gas. After this time, 1,2-dibromoethane (3 mL, 6.54 g, 0.035) was added to the reaction mixture and it was left to stir at 60°C overnight. After being cooled to room temperature, the reaction mixture was concentrated under reduced pressure to remove acetonitrile, diluted with ethyl acetate (60 mL) and then poured into a solution of saturated ammonium chloride (60 mL). The aqueous and organic layers were separated and then the aqueous layer was extracted further with ethyl acetate (2 × 60 mL). The combined organic layers were washed with brine (60 mL), dried over $MgSO_4$, and concentrated under reduced pressure. The crude reaction mixture was then subjected to flash column chromatography (5:95 → 10:90 ethyl acetate/hexanes) to give **(2)** as a white solid (409 mg, 20%). The spectroscopic data for compound **(2)** matched that reported previously in the literature.[31]

4-(1-(4-(2-(6-Aminohexylamino)ethoxy)phenyl)-2-phenylbut-1-enyl)phenol (3): **(2)** (188 mg, 0.44 mmol), 1,6-diaminohexane (1.88 g, 0.016 mol) and dry THF (7.5 mL) were combined in a sealed tube, and heated with stirring for 18 hours. After this time, the reaction mixture was cooled to room temperature and then fused to silica gel. The crude reaction mixture was then subjected to flash column chromatography (80:15:5 $CHCl_3$/MeOH/NH_4OH) to give **(3)** as an oil (132 mg, 65%). The spectroscopic data for compound **(3)** matched that reported previously in the literature.[31]

Conjugation of 4-(1-(4-(2-(6-Aminohexylamino)ethoxy)phenyl)-2-phenylbut-1-enyl)phenol with Alexa Fluor® 488 fluorophore (4): Commercially available Alexa Fluor® 488 succinimidyl ester (2 mg) was dissolved in dry DMSO (0.25 mL) and transferred to a flask containing **(3)** (10 mg) and dry DMSO (0.25 mL). The resulting mixture was left to stir at room temperature, under an atmosphere of argon gas, overnight, in the dark. After this time, the reaction mixture was purified *via* preparative HPLC (60:40 methanol/water, 55 minutes). The eluent also contained 0.1% trifluoroacetic acid. Analytical purity >99% by HPLC (retention time: 27.57 min). The fractions containing the appropriate product were concentrated under reduced pressure to remove acetonitrile and then freeze-dried using a lyophilizer to give a red solid (0.2 mg). Insufficient material was recovered to acquire a fully resolved NMR spectra. Details can be found in the supplementary information. **HRMS** (APCI): calc. for $C_{51}H_{49}N_4O_{12}S_2$ $[M + H]^+$ 973.2788, found 973.2805.

Conjugation of 4-(1-(4-(2-(6-Aminohexylamino)ethoxy)phenyl)-2-phenylbut-1-enyl)phenol with BODIPY fluorophore (5):

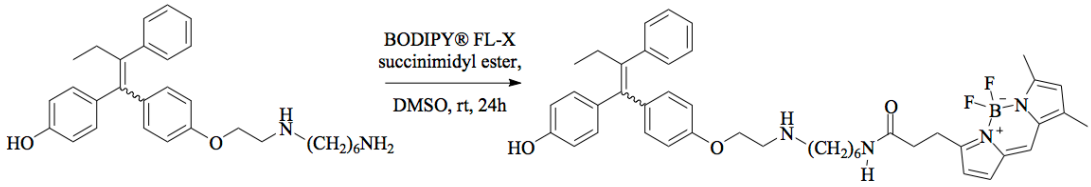

(3) **(5)**

Commercially available BODIPY® FL-X succinimidyl ester (5 mg) was dissolved in dry DMSO (0.25 mL) and transferred to a flask containing OHT-6C (10 mg) and dry DMSO (0.25 mL). The resulting mixture was left to stir at room temperature, under an atmosphere of argon gas, overnight, in the dark. After this time, the reaction mixture was purified *via* preparative HPLC (20:80 acetonitrile/water, 45 minutes → 100% acetonitrile, 15 minutes). The eluent also contained 0.1% trifluoroacetic acid. The fractions containing the appropriate product were concentrated under reduced pressure to remove acetonitrile and then freeze-dried using a lyophilizer to give a red solid (3 mg).The spectroscopic data for compound **(5)** matched that reported previously in the literature.[9] Briefly: **^{1}H NMR** (600.13 MHz, CD_3OD): δ= 7.43(1H, s), 7.18-6.99 (10H, m), 6.78 (1H, dd, J=8.7, 3.2 Hz), 6.40 (1H, d, J= 8.1 Hz), 6.32 (1H, t, J=4.2 Hz), 6.21 (1H, s), 3.46 (4H, br, m), 3.43-3.37 (2H, m), 3.21-3.17 (3H, m), 3.09 (1H, t, J=7.9 Hz), 3.02 (1H, t, J=7.9 Hz), 2.62-2.58 (2H, m), 2.51-2.42 (5H, m), δ 2.27 (3H, s), 1.77-1.65 (2H, m), 1.56-1.32 (7H, m), 0.88 (3H, t, J=7.7 Hz). Insufficient material was generated to obtain a 13C NMR. **HRMS** (ES): calc. for $C_{44}H_{52}BF_2N_4O_3$ $[M + H]^+$ 733.4022, found 733.4080; $C_{44}H_{51}BF_2N_4O_3Na$ $[M + Na]^+$ 755.3920 found 755.3928.

Cell culture and bioconjugate incubation: Breast cancer cells (ER positive MCF7 and ER negative MDA231) were cultured in RPMI media containing 10% fetal bovine serum (Life Technologies). Cells were grown at 37°C in a humidifying incubator and then were sub-cultured onto glass coverslips in sterile six-well plates at a concentration of 4 x10^5 cells/mL. Sub-confluent cultures were incubated for one hour in either **(4)** or **(5)** diluted in culture media to 10 µg/mL. Prior to imaging,

cultures were rinsed and replaced into normal growth media. Live stained cells were mounted under buffered saline and visualised using a Nikon A1Si fluorescent confocal microscope. Sequential fields were captured in the z-plane to confirm internal cellular localisation.

Imaging experiments

The imaging needle was fabricated as described in.[24] Briefly, the device consists of a length of double-clad fibre (SM-9/105/125-20A, Nufern, USA). The distal end is terminated with focusing optics fabricated by fusion-splicing a short section of large-core step-index fibre which serves as a beam-expanding spacer; a section of GRIN fibre (100/125 GIMM, Draka Communications, USA) which functions as a lens; and an angle-polished section of no-core fibre to redirect the light beam perpendicular to the fibre. This is enclosed within a small glass capillary to maintain a fibre-air interface at the angle polished surface and ensure total-internal reflection of the light beam. The fibre was inserted into a 23-gauge stainless steel needle (outer diameter 640μm) and aligned such that the light beam was directed out through a small hole that had been electrochemically etched into the side of the needle, and then glued in place using optical adhesive. The imaging needle was fusion spliced to a double-clad fibre coupler (Castor Optics, Canada), which allows the OCT light and fluorescence excitation to be inserted into the imaging needle, and backscattered OCT light and fluorescence emission to be separated upon return. OCT imaging was performed using a custom-built swept-source OCT system, based on a 50 kHz repetition rate, wavelength-swept laser source (Axsun Technologies Inc., USA). Fluorescence excitation used 488-nm wavelength light from a frequency-doubled semiconductor laser (Sapphire SF 488, Coherent Inc., USA). The fluorescence emission was detected using a photo-multiplier tube (PMT) (9136B, Electron Tubes, United Kingdom).

During imaging experiments, the imaging needle was mounted on a 2-axis motorized translation stage and positioned a few hundred microns above the coverslips that held the cell cultures. The needle was scanned parallel to the coverslip over a 5mm x 5mm field of view, with 4μm x 4μm spacing between measurements. OCT and fluorescence measurements were intrinsically co-registered as they were acquired simultaneously. Data was subsequently processed and visualised using in-house software developed in C++ and Matlab (MathWorks, USA).

Acknowledgements

The authors declare no conflict of interest. R.O.F. would like to thank Dr Anthony Reeder (CMCA-UWA) for help with mass spectra acquisition; Dr Gavin Flematti for assistance with HPLC and financial support by the Australian Research Council (DE180100112), Cancer Council Western Australia through a Susan Cavanagh ECI grant and the University of Western Australia ReEntry Fellowship. R.A.M. is supported by the Australian Research Council (CE140100003 and DP150104660); Breast Cancer Research Centre WA; and a Premier's Research and Industry Fund grant provided by the South Australian Government Department for Industry and Skills.

References

1. Specht, E. A.; Braselmann, E.; Palmer, A. E., A Critical and Comparative Review of Fluorescent Tools for Live-Cell Imaging. *Annual Review of Physiology* **2017,** *79* (1), 93-117.
2. Fu, Y.; Finney, N. S., Small-molecule fluorescent probes and their design. *RSC Advances* **2018,** *8* (51), 29051-29061.
3. Liu, H.-W.; Chen, L.; Xu, C.; Li, Z.; Zhang, H.; Zhang, X.-B.; Tan, W., Recent progresses in small-molecule enzymatic fluorescent probes for cancer imaging. *Chem. Soc. Rev.* **2018,** *47* (18), 7140-7180.
4. Jordan, V. C.; Koerner, S., Tamoxifen (ICI 46,474) and the human carcinoma 8S oestrogen receptor. *European Journal of Cancer (1965)* **1975,** *11* (3), 205-206.
5. O'Regan, R. M.; Jordan, V. C., The evolution of tamoxifen therapy in breast cancer: selective oestrogen-receptor modulators and downregulators. *The Lancet Oncology* **2002,** *3* (4), 207-214.
6. Jordan, V. C., Tamoxifen as the first targeted long-term adjuvant therapy for breast cancer. *Endocrine-Related Cancer* **2014,** *21* (3), R235-R246.
7. Shagufta; Ahmad, I., Tamoxifen a pioneering drug: An update on the therapeutic potential of tamoxifen derivatives. *European Journal of Medicinal Chemistry* **2018,** *143*, 515-531.
8. Maximov, P. Y.; McDaniel, R. E.; Jordan, V. C.; Maximov, P. Y.; McDaniel, R. E.; Jordan, V. C., *Tamoxifen: pioneering medicine in breast cancer*. Springer: 2013.
9. Rickert, E. L.; Oriana, S.; Hartman-Frey, C.; Long, X.; Webb, T. T.; Nephew, K. P.; Weatherman, R. V., Synthesis and Characterization of Fluorescent 4-Hydroxytamoxifen Conjugates with Unique Antiestrogenic Properties. *Bioconjugate Chem.* **2010,** *21* (5), 903-910.
10. Abendroth, F.; Solleder, M.; Mangoldt, D.; Welker, P.; Licha, K.; Weber, M.; Seitz, O., High Affinity Fluorescent Ligands for the Estrogen Receptor. *Eur. J. Org. Chem.* **2015,** *2015* (10), 2157-2166.
11. Ho, L. A.; Thomas, E.; McLaughlin, R. A.; Flematti, G. R.; Fuller, R. O., A new selective fluorescent probe based on tamoxifen. *Bioorg. Med. Chem. Lett.* **2016,** *26* (20), 4879-4883.
12. Yogo, T.; Umezawa, K.; Kamiya, M.; Hino, R.; Urano, Y., Development of an Activatable Fluorescent Probe for Prostate Cancer Imaging. *Bioconjugate Chem.* **2017,** *28* (8), 2069-2076.
13. Zhu, H.; Fan, J.; Du, J.; Peng, X., Fluorescent Probes for Sensing and Imaging within Specific Cellular Organelles. *Acc. Chem. Res.* **2016,** *49* (10), 2115-2126.
14. Blagg, J.; Workman, P., Choose and Use Your Chemical Probe Wisely to Explore Cancer Biology. *Cancer Cell* **2017,** *32* (1), 9-25.
15. Valdés, P. A.; Kim, A.; Brantsch, M.; Niu, C.; Moses, Z. B.; Tosteson, T. D.; Wilson, B. C.; Paulsen, K. D.; Roberts, D. W.; Harris, B. T., δ-aminolevulinic acid–induced protoporphyrin IX concentration correlates with histopathologic markers of malignancy in human gliomas: the need for quantitative fluorescence-guided resection to identify regions of increasing malignancy. *Neuro-Oncology* **2011,** *13* (8), 846-856.
16. Gabriele, M. L.; Wollstein, G.; Ishikawa, H.; Kagemann, L.; Xu, J.; Folio, L. S.; Schuman, J. S., Optical Coherence Tomography: History, Current Status, and Laboratory Work. *Invest Ophthalmol. Vis. Sci.* **2011,** *52* (5), 2425-2436.
17. Tearney, G. J.; Regar, E.; Akasaka, T.; Adriaenssens, T.; Barlis, P.; Bezerra, H. G.; Bouma, B.; Bruining, N.; Cho, J.-m.; Chowdhary, S.; Costa, M. A.; de Silva,

R.; Dijkstra, J.; Di Mario, C.; Dudeck, D.; Falk, E.; Feldman, M. D.; Fitzgerald, P.; Garcia, H.; Gonzalo, N.; Granada, J. F.; Guagliumi, G.; Holm, N. R.; Honda, Y.; Ikeno, F.; Kawasaki, M.; Kochman, J.; Koltowski, L.; Kubo, T.; Kume, T.; Kyono, H.; Lam, C. C. S.; Lamouche, G.; Lee, D. P.; Leon, M. B.; Maehara, A.; Manfrini, O.; Mintz, G. S.; Mizuno, K.; Morel, M.-a.; Nadkarni, S.; Okura, H.; Otake, H.; Pietrasik, A.; Prati, F.; Räber, L.; Radu, M. D.; Rieber, J.; Riga, M.; Rollins, A.; Rosenberg, M.; Sirbu, V.; Serruys, P. W. J. C.; Shimada, K.; Shinke, T.; Shite, J.; Siegel, E.; Sonada, S.; Suter, M.; Takarada, S.; Tanaka, A.; Terashima, M.; Troels, T.; Uemura, S.; Ughi, G. J.; van Beusekom, H. M. M.; van der Steen, A. F. W.; van Es, G.-A.; van Soest, G.; Virmani, R.; Waxman, S.; Weissman, N. J.; Weisz, G., Consensus Standards for Acquisition, Measurement, and Reporting of Intravascular Optical Coherence Tomography Studies: A Report From the International Working Group for Intravascular Optical Coherence Tomography Standardization and Validation. *J. Am. Coll. Cardiol.* **2012,** *59* (12), 1058-1072.

18. Suter, M. J.; Nadkarni, S. K.; Weisz, G.; Tanaka, A.; Jaffer, F. A.; Bouma, B. E.; Tearney, G. J., Intravascular optical imaging technology for investigating the coronary artery. *JACC Cardiovasc Imaging* **2011,** *4* (9), 1022-1039.

19. Huang, D.; Swanson, E. A.; Lin, C. P.; Schuman, J. S.; Stinson, W. G.; Chang, W.; Hee, M. R.; Flotte, T.; Gregory, K.; Puliafito, C. A.; et, a., Optical coherence tomography. *Science* **1991,** *254* (5035), 1178.

20. Scolaro, L.; McLaughlin, R.A.; Kennedy, B.F.; Saunders, C. M.; Sampson, D, D., A review of optical coherence tomography in breast cancer. *Photonics & Lasers in Medicine* **2014,** *3* (3), 225.

21. Wang, R. K., Signal degradation by multiple scattering in optical coherence tomography of dense tissue: a Monte Carlo study towards optical clearing of biotissues. *Phys. Med. Biol.* **2002,** *47* (13), 2281-2299.

22. Welzel, J., Optical coherence tomography in dermatology: a review. *Skin Res. Technol.* **2001,** *7* (1), 1-9.

23. Lorenser, D.; Quirk, B. C.; Auger, M.; Madore, W.-J.; Kirk, R. W.; Godbout, N.; Sampson, D. D.; Boudoux, C.; McLaughlin, R. A., Dual-modality needle probe for combined fluorescence imaging and three-dimensional optical coherence tomography. *Opt. Lett.* **2013,** *38* (3), 266-268.

24. Scolaro, L.; Lorenser, D.; Madore, W.-J.; Kirk, R. W.; Kramer, A. S.; Yeoh, G. C.; Godbout, N.; Sampson, D. D.; Boudoux, C.; McLaughlin, R. A., Molecular imaging needles: dual-modality optical coherence tomography and fluorescence imaging of labeled antibodies deep in tissue. *Biomed Opt Express* **2015,** *6* (5), 1767-1781.

25. Scolaro, L.; Lorenser, D.; McLaughlin, R. A.; Quirk, B. C.; Kirk, R. W.; Sampson, D. D., High-sensitivity anastigmatic imaging needle for optical coherence tomography. *Opt. Lett.* **2012,** *37* (24), 5247-5249.

26. Dillon, M. F.; Hill, A. D. K.; Quinn, C. M.; McDermott, E. W.; O'Higgins, N., A Pathologic Assessment of Adequate Margin Status in Breast-Conserving Therapy. *Annals of Surgical Oncology* **2006,** *13* (3), 333-339.

27. Yu, D. D.; Forman, B. M., Simple and Efficient Production of (Z)-4-Hydroxytamoxifen, a Potent Estrogen Receptor Modulator. *The Journal of Organic Chemistry* **2003,** *68* (24), 9489-9491.

28. Shiau, A. K.; Barstad, D.; Loria, P. M.; Cheng, L.; Kushner, P. J.; Agard, D. A.; Greene, G. L., The Structural Basis of Estrogen Receptor/Coactivator Recognition and the Antagonism of This Interaction by Tamoxifen. *Cell* **1998,** *95* (7), 927-937.

29. Katzenellenbogen, J. A.; Carlson, K. E.; Katzenellenbogen, B. S., Facile geometric isomerization of phenolic non-steroidal estrogens and antiestrogens: Limitations to the interpretation of experiments characterizing the activity of individual isomers. *Journal of Steroid Biochemistry* **1985,** *22* (5), 589-596.
30. Gottlieb, H. E.; Kotlyar, V.; Nudelman, A., NMR Chemical Shifts of Common Laboratory Solvents as Trace Impurities. *The Journal of Organic Chemistry* **1997,** *62* (21), 7512-7515.
31. Trebley, J. P.; Rickert, E. L.; Reyes, P. T.; Weatherman, R. V. In *Tamoxifen-Based Probes for the Study of Estrogen Receptor-Mediated Transcription*, Chemical Genomics, Berlin, Heidelberg, 2006//; Jaroch, S.; Weinmann, H., Eds. Springer Berlin Heidelberg: Berlin, Heidelberg, 2006; pp 75-87.